Robotica (2008) volume 26, pp. 277–283. © 2007 Cambridge University Press
doi:10.1017/S0263574707003888 Printed in the United Kingdom

Global ultrasonic system with selective activation for autonomous navigation of an indoor mobile robot

Soo-Yeong Yi*

Department of Electrical Engineering, Seoul National University of Technology, Seoul, South Korea

(Received in Final Form: August 12, 2007. First published online: September 28, 2007)

SUMMARY

This paper presents a global ultrasonic system with selective activation algorithm for autonomous navigation of an indoor mobile robot. The global ultrasonic system consists of several ultrasonic transmitters fixed at reference positions in global coordinates and two receivers at moving coordinates of a mobile robot. By activating the ultrasonic transmitters through an radiofrequency (RF) channel, the robot is able to obtain distance information to the reference positions and localize itself in the global coordinates. Due to limitations in signal strength and beam width, the ultrasonic signals from some transmitters may not be delivered to the robot and the ultrasonic data become invalid. In order to improve the effectiveness of the global ultrasonic system, a so-called selective activation algorithm is developed. Based on the current position of the robot, the selective activation calls a proper ultrasonic transmitter and generates valid ultrasonic data at every sampling instant, resulting in faster, more accurate response for self-localization than does simple sequential activation. Path-following control experiments are conducted to verify the effectiveness of the self-localization based on the proposed selective activation algorithm with the global ultrasonic system.

KEYWORDS: Selective activation; Global ultrasonic system; Extended Kalman filter; Self-localization.

1. Introduction

For autonomous navigation in a workspace, a mobile robot should be able to identify its location and the direction in which it is moving, that is, its self-localization. Self-localization capability is the most basic requirement of a mobile robot, since it is the basis for on-line trajectory planning and control.[1] Self-localization methods can be classified into local and global methods. In local methods, a mobile robot localizes itself by making a local object map and matching it with a given global map database. This local object map requires the relative distances to all surrounding objects in moving coordinate of the mobile robot. Therefore, the local method demands massive computation in the map-making and matching processes. In an extreme case, the robot has to stop moving momentarily to obtain the necessary environmental information.[2] By contrast, the global method localizes quickly and efficiently, requiring distance measurements from only three or more reference positions in the global coordinates; it avoids the time-consuming map-making and matching processes.

Several kinds of sensors have been used for range measurement of the self-localization, e.g., camera vision, laser distance sensor, infrared sensor, radio frequency wave, and ultrasonic sensor. The conventional landmark technique[3] for the camera vision and the so-called active badge system[4] using the infrared sensors are classified into the global localization method. The global localization method is better exemplified by the well-known satellite Global Positioning System (GPS) used for ground vehicles, ships, and so on.[5]

In order to take advantage of the GPS for indoor applications, pseudo-lite localization systems were proposed by using the radio frequency transmitters or ultrasonic transmitters. Cobb[6] developed the pseudo-lite system using the radio frequency transmitters and Kee[7] applied the pseudo-lite system for navigation of an indoor mobile robot. The pseudo-lite system using the radio frequency transmitters requires highly accurate and expensive electronic drivers for range measurement. Thus, in practical point of view, it is understood that the ultrasonic sensor is more simple and cost-effective than the radio frequency transmitter for indoor applications.

The ultrasonic pseudo-lite systems are also known as active beacon systems in comparison with conventional passive beacon systems.[8,9] As an active ultrasonic beacon system, Kleeman[10] proposed a positioning system with ultrasonic transmitters (TSs) fixed at *a priori* known positions in the workspace and an ultrasonic receiver (RS) array on the mobile robot. This system requires a burdensome external supervisory controller and a wired connection between the TSs. Moreover, the timing between TS and RS for time-of-flight (TOF) measurements is vulnerable, as it relies only on inherent timers. Recently, similar ultrasonic localization system called Hexmite system[11] was commercialized. The Home Robot Positioning System (HRPS)[16] has inverse structure as one TS on a mobile robot and several RSs at fixed points in workspace. The infrared signal is used as trigger for the ultrasonic receivers to measure the TOF of ultrasonic signal from the transmitter in the HRPS.

For human localization in the ubiquitous computing environment, the Cricket system[12] was proposed. The Cricket system has a radiofrequency (RF) channel as well as ultrasonic channel, that is, the TSs have a RF-transmitter (TX) and the moving objects have RF receiver (RX), as well as the RS. The RF channel was used to synchronize the TS

* Corresponding author. E-mail: suylee@snut.ac.kr

and RS in the TOF measurement in this case since the RF signal is much faster than the ultrasonic signal. In the previous ultrasonic approaches,[10–12] the moving object is passive in generation of the ultrasonic signal and only receives the signal. By contrast, the global ultrasonic system consists of TSs with RX in the workspace, and two RSs with a TX on the mobile robot. Therefore, by using the TX, the robot is able to control the generation of the ultrasonic signal actively.[13]

Due to its signal strength and the beam width, the ultrasonic signal has limitations in terms of the detectable distance and area. Therefore, the number of TSs should be increased to cover the entire workspace. When using multiple TSs together in a system, the activation scheme for the TSs has crucial effects on the overall localization performance. To minimize the interference between ultrasonic signals, the active beacon system[10] used simple sequential activation, and the Cricket location system used random activation.[12] In simple sequential and random activation, however, the signal may not be delivered to the robot due to the limitations in the ultrasonic signal, thereby, many sampling instants can be voided and the overall localization performance degraded.

This paper proposes a new activation scheme for the global ultrasonic system called selective activation. The selective activation considers the measurability of ultrasonic signals at the position of a mobile robot. Therefore, the number of valid ultrasonic data increases at the robot, improving the corresponding localization and navigation performance.

In the following, Section 2 presents an overview of the global ultrasonic system. The selective activation scheme and the extended Kalman filter ultrasonic data processing algorithms are presented in Section 3 and 4, respectively. Section 5 presents experimental results for selective activation, including a comparison with conventional sequential activation. Concluding remarks are presented in Section 6.

2. The Global Ultrasonic System*

As depicted in Fig. 1, the global ultrasonic system has some TSs at fixed reference positions, $\boldsymbol{T}_i = [x_i\ y_i\ z_i]^t$ in world coordinates, and front and rear RSs, $\boldsymbol{p}_f$ and $\boldsymbol{p}_r$ in the moving coordinates of a mobile robot. The subscript i denotes the index of TSs in the system. With respect to the center of the robot, $\boldsymbol{p} = [x, y, z_c]^t$, the positions of the two RSs, $\boldsymbol{p}_f$ and $\boldsymbol{p}_r$, are given as

$$\boldsymbol{p}_f = \begin{bmatrix} x + l\cos\theta \\ y + l\sin\theta \\ z_c \end{bmatrix}, \quad \boldsymbol{p}_r = \begin{bmatrix} x - l\cos\theta \\ y - l\sin\theta \\ z_c \end{bmatrix} \tag{1}$$

where l is a baseline from the center of robot to an RS and θ denotes the heading angle of the robot. Without loss of generality, the moving surface is assumed to be flat and the z component of the position vectors is a constant, z_c.

In the case of several independent TSs together in a system, the following issues should be considered:

(1) Cross-talk between ultrasonic signals.
(2) The identification of each ultrasonic signal.

* This section of the paper is summarized from the work of Yi and Choi.[13]

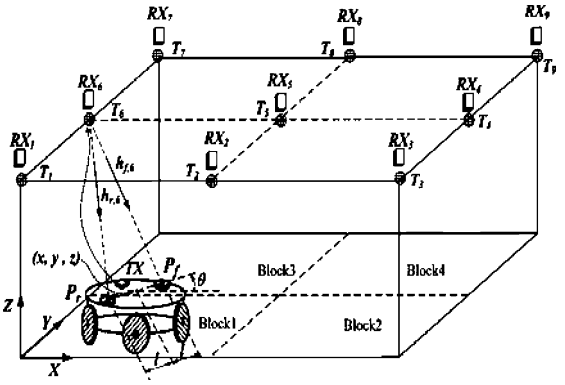

Fig. 1. The global ultrasonic system with nine TSs: h_f, i and h_r, i denote the external distances from $\boldsymbol{p}_f$ and $\boldsymbol{p}_r$ to $\boldsymbol{T}_i$, respectively.

(3) The synchronization between TS and RS, which is needed to measure the TOF of the ultrasonic signal.

To address these issues, RF modules (RXs and TXs) are added to the ultrasonic sensors, as shown in Fig. 1. The robot then calls to activate one of the TSs, through the RF channel, for each time slot. Assuming that the delivery time for the RF calling signal is ignored, the ultrasonic signal generation at $\boldsymbol{T}_i$ occurs simultaneously with the RF signal transmission from TX on the robot. Therefore, it is possible to synchronize the TS and RS pair and to obtain distance between them by counting the TOF of the ultrasonic signal. Based on the distance information to some TSs at the reference points, the robot is able to localize itself in the global coordinates.

3. Algorithm for Selective Activation

The appropriate number of TSs depends on the size of the workspace. Based on the current estimation of the robot position, the selective activation scheme chooses a proper TS to activate, considering the detectable range and beam width of the ultrasonic signal.

3.1. Selective activation according to distance

A simple criterion for selective activation, based on the detectable distance of an ultrasonic signal, can be described as

$$T_{dist} = \{T_i \,|\, \|T_i - \hat{p}\| < D_{th},\ i = 1,\ 2,\ \ldots,\ N\} \tag{2}$$

where $\|\cdot\|$ denotes the distance of a vector "$\cdot$", D_{th} represents the threshold of the distance given from the specification of ultrasonic transducer, and $\hat{\boldsymbol{p}}$ is the current estimation of the robot position. The SRF04 ultrasonic transducer adopted in this paper has $3\,m$ as D_{th}.[14] Note that the position of robot, $\hat{\boldsymbol{p}}$, is used in Eq. (2), instead of the position of the RS, $\hat{\boldsymbol{p}}_f$ or $\hat{\boldsymbol{p}}_r$. Since the difference in length from $\hat{\boldsymbol{p}}$ to $\hat{\boldsymbol{p}}_f$ or $\hat{\boldsymbol{p}}_r$ is negligible in comparison with the ultrasonic distance, $\|T_i - \hat{\boldsymbol{p}}\|$ is approximately equal to $\|\boldsymbol{T}_i - \hat{\boldsymbol{p}}_f\|$ or $\|\boldsymbol{T}_i - \hat{\boldsymbol{p}}_r\|$.

To simplify the distance computation, the distance-based criterion in Eq. (2) is modified to the block-based criterion. The TSs are grouped in blocks in advance, as illustrated in Fig. 1. When the robot is inside of a block, only a TS in the block is activated. In Fig. 1, criterion for the block-based

https://doi.org/10.1017/S0263574707003888 Published online by Cambridge University Press

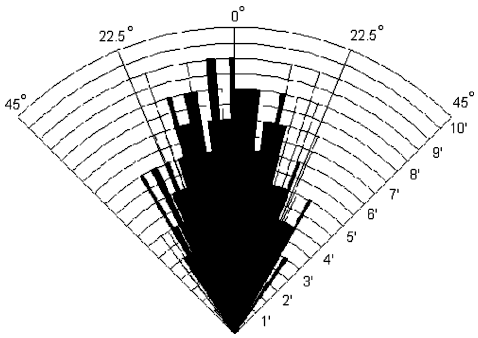

Fig. 2. Beam width of the SRF04 ultrasonic sensor.

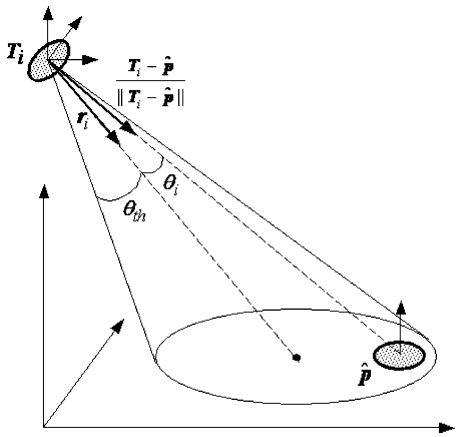

Fig. 3. Selection based on beam width.

activation can be described as

$$T_{block} = \begin{cases} \{T_1, T_2, T_5, T_6\} & \text{if } \hat{p} \in \text{Block 1} \\ \{T_2, T_3, T_4, T_5\} & \text{if } \hat{p} \in \text{Block 2} \\ \{T_5, T_6, T_7, T_8\} & \text{if } \hat{p} \in \text{Block 3} \\ \{T_4, T_5, T_8, T_9\} & \text{if } \hat{p} \in \text{Block 4} \end{cases} \tag{3}$$

In case that there are many TSs in wide work area, the block-based criterion is helpful to reduce the computation time.

3.2. Selective activation according to beam width

The limitation on the beam width can restrict the delivery of the ultrasonic signal to RS, although the receiver seems close enough. Figure 2, shows the beam width of SRF04.[14]

It is assumed that the RSs on the robot are vertically upward, and the unit normal vector of TS is given by r_i, as in Fig. 3. The angle between r_i and the direction vector from the TS to the robot can be described as

$$\theta_i = \cos^{-1}\left(\frac{T_i - \hat{p}}{\|T_i - \hat{p}\|} \cdot r_i\right) \tag{4}$$

where "·" denotes the vector inner product. The activation criterion can be represented as

$$T_{angle} = \{T_i \,|\, |\theta_i| < \theta_{th},\ i = 1, 2, \ldots, N\} \tag{5}$$

where θ_{th} is the threshold value of the beam width given by the specification of the ultrasonic transducer. As in Fig. 2, θ_{th} for the SRF04 is approximately 23°.

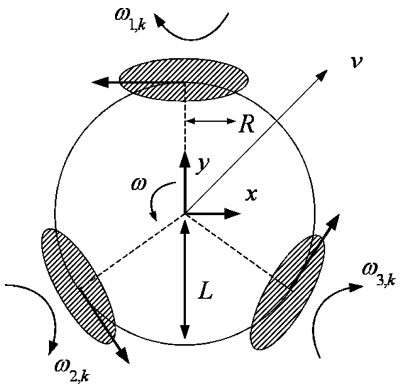

Fig. 4. Mobile robot with three omnidirectional wheels.

4. Extended Kalman Filter for Self-localization

The well-known Kalman filter is used to combine the external distance data with the internal encoder data of the mobile robot, thereby obtaining the position and heading angle of the robot in global coordinates.[10,15]

The internal state equation of the omnidirectional mobile robot in Fig. 4 is written as

$$\begin{bmatrix} x_{k+1} \\ y_{k+1} \\ \theta_{k+1} \end{bmatrix} = \begin{bmatrix} x_k \\ y_k \\ \theta_k \end{bmatrix} + \frac{T \cdot R}{3} \begin{bmatrix} -2 & 1 & 1 \\ 0 & -\sqrt{3} & \sqrt{3} \\ 1/L & 1/L & 1/L \end{bmatrix} \begin{bmatrix} \omega_{1,k} \\ \omega_{2,k} \\ \omega_{3,k} \end{bmatrix} \tag{6}$$

where the subscript k denotes time index, T is the sampling interval, $\omega_{1,k}$, $\omega_{2,k}$, and $\omega_{3,k}$ represent the angular velocities of each wheel of the robot, and L and R are the radii of the robot body and wheel.

Using (1) and (6), the motion of the front RS mounted on the robot can be described by the following equations:

$$\begin{aligned} p_{f,k+1} &= f_f(p_{f,k}, u_k, q_k) \\ &= \begin{bmatrix} x_{f,k} + \frac{TR}{3}(-2\omega_{1,k} + \omega_{2,k} + \omega_{3,k}) \\ \quad + l\cos\left\{\theta_k + \frac{TR}{3L}(\omega_{1,k} + \omega_{2,k} + \omega_{3,k})\right\} \\ \quad - l\cos\theta_k + q_{1,k} \\ y_{f,k} + \frac{TR}{3}(-\sqrt{3}\omega_{2,k} + \sqrt{3}\omega_{3,k}) \\ \quad + l\sin\left\{\theta_k + \frac{TR}{3L}(\omega_{1,k} + \omega_{2,k} + \omega_{3,k})\right\} \\ \quad - l\sin\theta_k + q_{2,k} \end{bmatrix} \end{aligned} \tag{7}$$

where $p_f = [x_f \quad y_f]^t$ denotes the position of the front RS on the $x - y$ plane, $u_k = [\omega_{1,k} \quad \omega_{2,k} \quad \omega_{3,k}]^t$ is the control input, and $q_k = [q_{1,k} \quad q_{2,k}]^t$ represents Gaussian noise with mean zero and variance Q. The external measurement equation at p_f is given as follows:

$$\begin{aligned} z_{f,k} &= h_f(p_{f,k}, v_k) \\ &= \left\{(x_{f,k} - x_i)^2 + (y_{f,k} - y_i)^2 + (z_c - z_i)^2\right\}^{1/2} + v_k \end{aligned} \tag{8}$$

https://doi.org/10.1017/S0263574707003888 Published online by Cambridge University Press

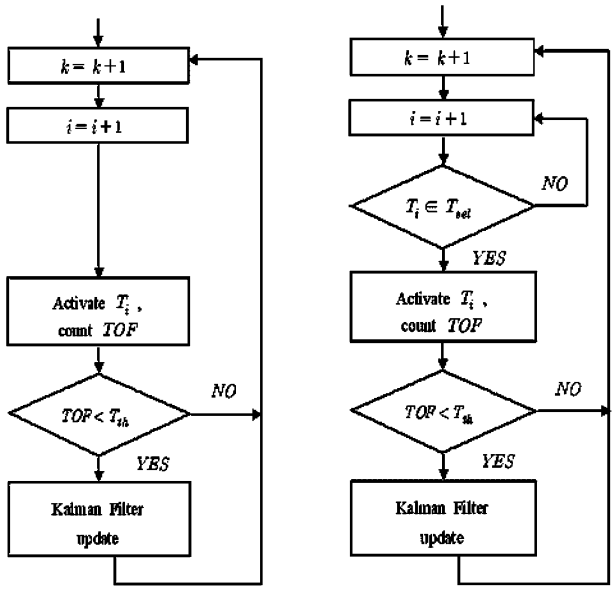

(a) Sequential activation (b) Selective activation

Fig. 5. Algorithm flow chart.

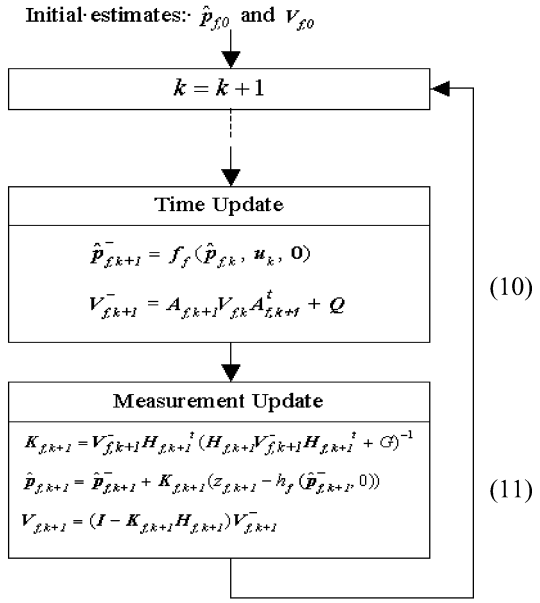

Fig. 6. The extended Kalman filter.

where v_k represents Gaussian noise with mean zero and variance G. The subscript i denotes the index of the TS in the set (9), according to the selective activation.

$$\boldsymbol{T}_{sel}(\hat{\boldsymbol{p}}) = \left\{ \boldsymbol{T}_i | \boldsymbol{T}_i \in \boldsymbol{T}_{block} \cap \boldsymbol{T}_{angle},\ i = 1, \ldots, n \right\} \quad (9)$$

The selective activation flowchart is compared with simple sequential activation in Fig. 5. Note that only the valid ultrasonic data delivered within an expected time interval have an effect on the self-localization through the Kalman filter. The validity of the ultrasonic data can be determined based on the TOF threshold value $\boldsymbol{T}_{th}$.

The extended Kalman filter for the front RS described by the state equation (7) and the measurement equation (8) can be written as Fig. 6.[15]

Fig. 6, $\hat{\boldsymbol{p}}^-_{f,k}$ and $\hat{\boldsymbol{p}}_{f,k}$ are *a priori* and *a posteriori* estimations for $\boldsymbol{p}_{f,k}$, and $\boldsymbol{V}_{f,k}{}^-$ and $\boldsymbol{V}_{f,k}$ are the error covariance matrices. The matrix $\boldsymbol{K}_{f,k+1}$ is the gain of the Kalman filter. The Jacobian matrices, $\boldsymbol{A}_{f,k+1}$ and $\boldsymbol{H}_{f,k+1}$ are described as follows:

$$\boldsymbol{A}_{f,k+1} = \frac{\partial\, f_f(\hat{\boldsymbol{p}}_{f,k}, \boldsymbol{u}_k, \boldsymbol{0})}{\partial\, \boldsymbol{p}_f} = \begin{bmatrix} 1 & 0 \\ 0 & 1 \end{bmatrix} \quad (12)$$

$$\boldsymbol{H}_{f,k+1} = \frac{\partial\, h_f(\hat{\boldsymbol{p}}^-_{f,k+1}, \boldsymbol{0})}{\partial\, \boldsymbol{p}_f} = \begin{bmatrix} \dfrac{\hat{x}^-_{f,k+1} - x_i}{D_{f,i}} & \dfrac{\hat{y}^-_{f,k+1} - y_i}{D_{f,i}} \end{bmatrix} \quad (13)$$

where

$$D_{f,i} = \{(\hat{x}^-_{f,k+1} - x_i)^2 + (\hat{y}^-_{f,k+1} - y_i)^2 + (z_c - z_i)^2\}^{1/2} \quad (14)$$

It is noted that $\hat{\boldsymbol{p}}_{f,0}$ and $\boldsymbol{V}_{f,0}$ should be given at the beginning and those values are near enough to the actual values for local convergence of the estimation process.

Although not shown here, similar equations for $\hat{\boldsymbol{p}}_{r,k}$ can be obtained by applying the same procedures used in Eqs. (7) through (14).

Using $\hat{\boldsymbol{p}}_{f,k}$ and $\hat{\boldsymbol{p}}_{r,k}$, the estimations of robot posture, including its position and heading angle, are obtained as

$$\hat{x}_k = \frac{\hat{x}_{f,k} + \hat{x}_{r,k}}{2}$$

$$\hat{y}_k = \frac{\hat{y}_{f,k} + \hat{y}_{r,k}}{2} \quad (15\text{-}1)$$

$$\hat{\theta}_k = \tan^{-1} \frac{\hat{y}_{f,k} - \hat{y}_{r,k}}{\hat{x}_{f,k} - \hat{x}_{r,k}} \quad (15\text{-}2)$$

Assuming that the error covariances for $\hat{\boldsymbol{p}}_{f,k}$ and $\hat{\boldsymbol{p}}_{r,k}$ are the same, the error covariances of the robot position and the heading angle estimation, as shown in Fig. 7, can be

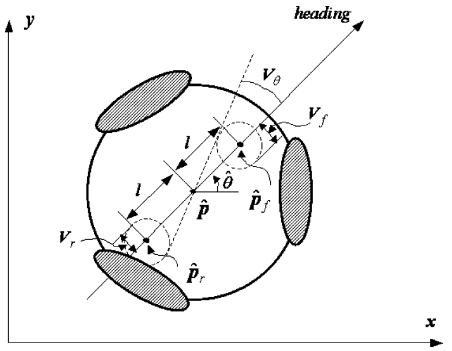

Fig. 7. Error covariances of the posture estimation.

https://doi.org/10.1017/S0263574707003888 Published online by Cambridge University Press

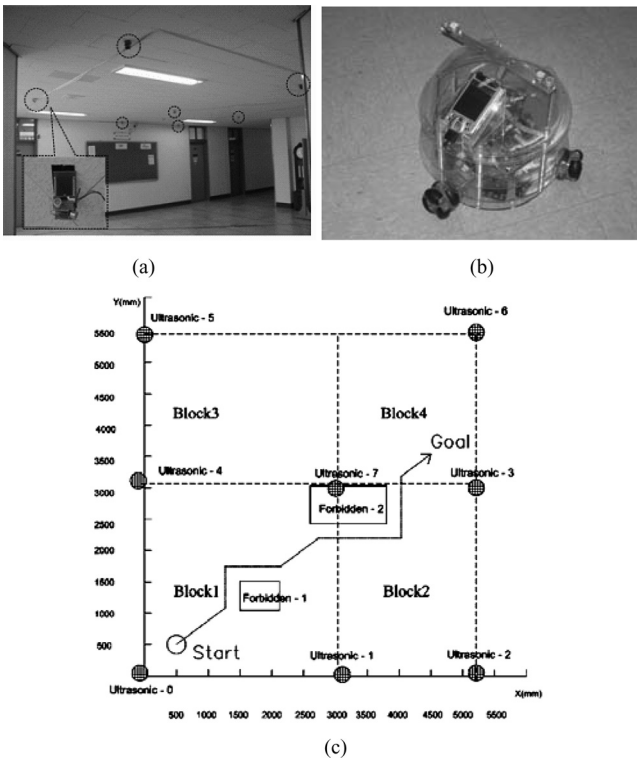

Fig. 8. Experimental setup: (a) Experimental workplace, (b) Omnidirectional mobile robot, and (c) Layout of ultrasonic transmitters.

calculated as:

$$\begin{aligned} \boldsymbol{V}_{p,k} &= \boldsymbol{E}\left[(\boldsymbol{r}-\hat{\boldsymbol{r}}_k)(\boldsymbol{r}-\hat{\boldsymbol{r}}_k)^2\right] \\ &= \boldsymbol{V}_{f,k}\ (=\boldsymbol{V}_{r,k}) \\ \boldsymbol{V}_{\theta,k} &= \boldsymbol{E}\left[(\theta-\theta_k)^2\right] \\ &\approx \tan^{-1}\frac{\boldsymbol{V}_{f,k}}{l} \end{aligned} \tag{16}$$

Equation (16) implies that the accuracy of the estimation of the heading angle depends on the baseline, l.

5. Experiments and Discussion

In order to verify the selective activation of the global ultrasonic system, eight TSs were established in an experimental workspace 2,600 mm high, 5,200 mm long, and 5,400 mm wide (see Fig. 8(a)). Figure 8(b) shows the omnidirectional mobile robot, where the baseline from the robot center to an RS is $l = 133$ mm. The layout of the TSs in the workspace and the block are depicted in Fig. 8(c). Experiments examining the path-following control based on the self-localization were carried out to investigate the effectiveness of the selective activation.

The mobile robot is controlled to follow the preplanned command path depicted in Fig. 8(c) from an initial posture, $(x_s,\ y_s,\ \theta_s) = (500,\ 500,\ 0)$ to a goal posture at $(x_g,\ y_g,\ \theta_g) = (4500,\ 3500,\ \pi/2)$. From Eq. (6), control input to the mobile robot can be written as

$$\begin{bmatrix}\omega_{1,k}\\ \omega_{2,k}\\ \omega_{3,k}\end{bmatrix} = \frac{3}{T\cdot R}\begin{bmatrix}-2 & 1 & 1\\ 0 & -\sqrt{3} & \sqrt{3}\\ 1/L & 1/L & 1/L\end{bmatrix}^{-1}\cdot\left(\begin{bmatrix}x^c_{k+1}\\ y^c_{k+1}\\ \theta^c_{k+1}\end{bmatrix}-\begin{bmatrix}\hat{x}_k\\ \hat{y}_k\\ \hat{\theta}_k\end{bmatrix}\right) \tag{17}$$

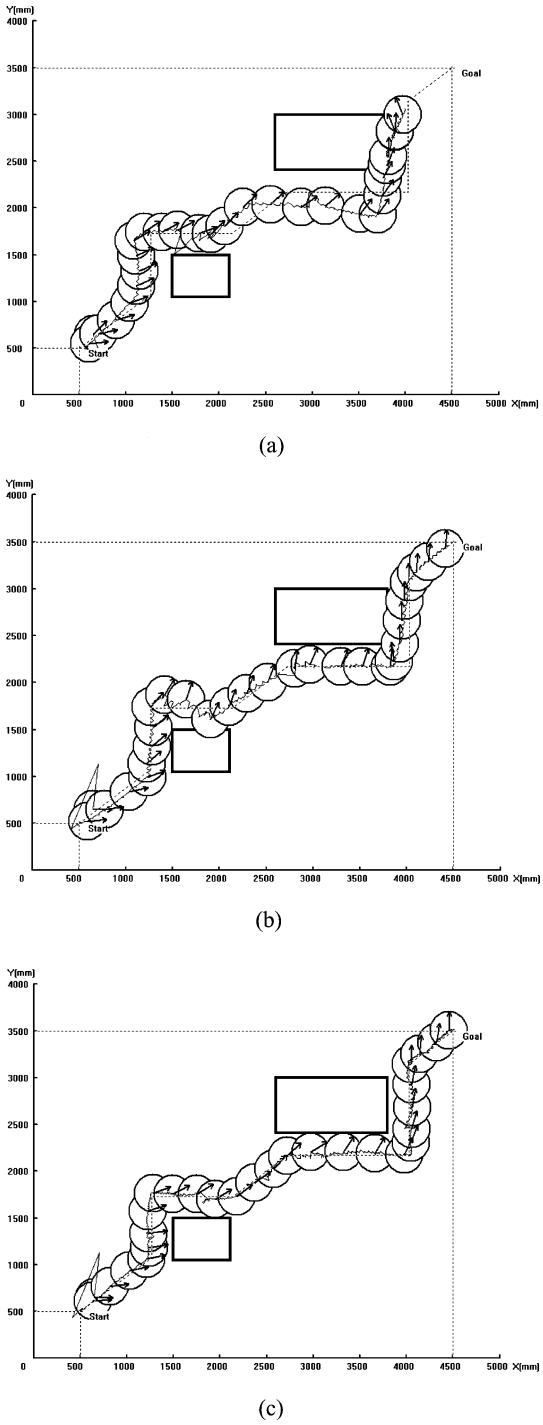

Fig. 9. Result of experiment: (a) Navigation by dead-reckoning, (b) Path-following control with global ultrasonic system by sequential activation, and (c) Path-following control with global ultrasonic system by selective activation.

where $[x^c_{k+1}\ y^c_{k+1}\ \theta^c_{k+1}]^t$ and $[\hat{x}_k\ \hat{y}_k\ \hat{\theta}_k]^t$ denote a command posture, and an estimated posture respectively. As the estimated posture, the path-following control takes use of *a posteriori* estimation (Eq. (11)), whereas the dead-reckoning navigation uses only *a priori* estimation (Eq. (10)) without the self-localization.

The results are depicted in Fig. 9, in which the bold rectangles represent regions forbidden by virtual obstacles and the dotted and continuous lines imply the command

https://doi.org/10.1017/S0263574707003888 Published online by Cambridge University Press

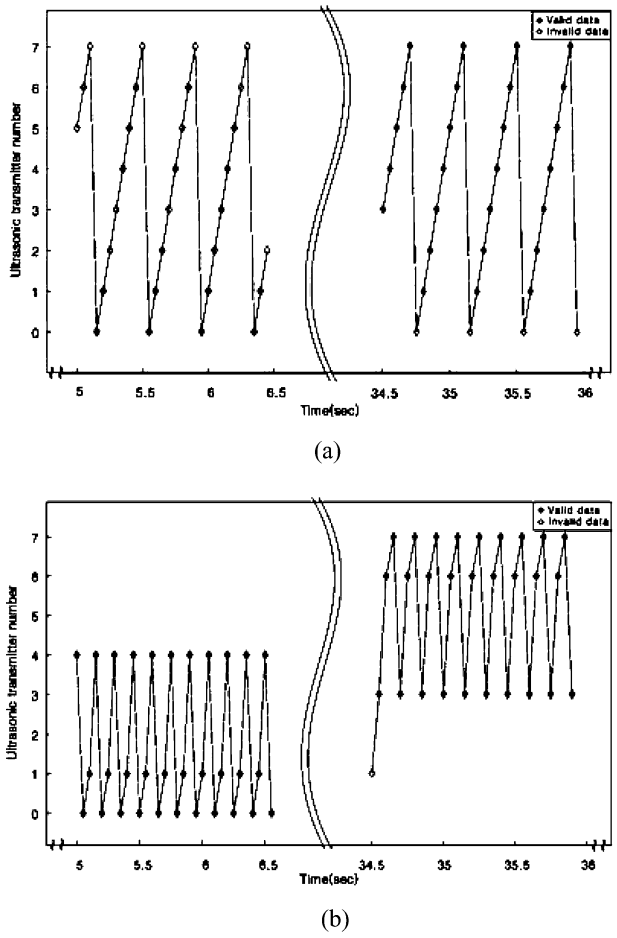

Fig. 10. Comparison of the valid ultrasonic data: (a) Sequential activation and (b) Selective activation.

and actual paths, respectively. The arrow at each circle represents the heading direction of the robot. Figure 9 also presents the result of dead-reckoning navigation for comparison. In the experiment of the dead-reckoning navigation, the global ultrasonic system is used to measure the actual position and heading angle of the robot. As depicted in Fig. 9(a), the dead-reckoning navigation of the mobile robot violates the forbidden regions. Therefore, the robot cannot reach its goal due to its modeling error and wheel slippage. The sequential activation example presented in Fig. 9(b) shows the relatively large deviation between the command and actual paths due to the lagged localization from many invalid ultrasonic data. Conversely, in the selective activation shown in Fig. 9(c), the robot successfully achieved the path-following control, since almost every sampling instant has valid ultrasonic data.

Figure 10 compares the valid ultrasonic data in the sequential and the selective activation scheme during the path-following control. In the sequential activation in Fig. 10(a), all the TSs established in the workspace are activated blindly without considering the measurability of the ultrasonic signals. However, in the selective activation, the set of TSs activated depends on the robot position. This can be seen in Fig. 10(b), where $\{\boldsymbol{T}_0, \boldsymbol{T}_1, \boldsymbol{T}_4\}$ is activated in the initial period and $\{\boldsymbol{T}_3, \boldsymbol{T}_6, \boldsymbol{T}_7\}$ in the final. Note that the initial position of the robot, (500, 500) shown in Fig. 8(c), belongs to Block 1, and the corresponding set of TSs is $\boldsymbol{T}_{block,1} = \{\boldsymbol{T}_0, \boldsymbol{T}_1, \boldsymbol{T}_4, \boldsymbol{T}_7\}$. The goal position, (4500, 3500), belongs to Block 4, and the corresponding set of TSs is $\boldsymbol{T}_{block,4} = \{\boldsymbol{T}_3, \boldsymbol{T}_6, \boldsymbol{T}_7\}$. The selection criterion, according to the beam width, excludes $\boldsymbol{T}_7$ in the initial period, although $\boldsymbol{T}_7$ belongs to Block 1. As a consequence, the selective activation scheme has much more valid data than the sequential activation, resulting in faster localization. The selection depends on the estimated position of the robot, not the actual position, therefore, there may also be some invalid ultrasonic data in selective activation, as shown in Fig. 10(b).

There are some sources of error in the localization based on the proposed global ultrasonic system: error in counting the TOF of ultrasonic signal, variation in speed of ultrasonic signal due to temperature change, uncertainty in position of each ultrasonic transmitter and linearization error in the extended Kalman filter. Among them, the position uncertainty of each ultrasonic transmitter mostly influences the localization error since it is hard to obtain the position coordinate of each ultrasonic transmitter installed in workspace. However, the localization error is acceptable in comparison with size of the mobile robot as shown in the results of experiment.

6. Conclusion

The global ultrasonic system is a kind of pseudo-lite GPS using ultrasonic transmitters fixed at reference positions in the workspace to enable self-localization of an indoor mobile robot. The robot's ability to control the generation and synchronization of the ultrasonic signal using an RF channel is the distinct feature of the global ultrasonic system versus the conventional active beacon system. This yields autonomy, and hence is capable of overcoming the demerits of the ultrasonic signals alone. Limitations on the measurable distance and beam width create many invalid ultrasonic data in the simple sequential activation scheme. Therefore, the performance of self-localization is greatly improved by being able to choose and activate a proper ultrasonic transmitter at each sampling instant according to the current position of the robot. This paper described a selective activation algorithm based on the detectable range and beam angle of ultrasonic signal. It is obvious that the selective activation becomes more effective as the number of ultrasonic transmitters is increased in the workspace.

In order to verify effectiveness of the selective activation algorithm, an experimental system including 8 ultrasonic transmitters and an omnidirectional mobile robot was established in this paper. Since an omnidirectional mobile robot is free of the well-known nonholonomic constraint, it is more appropriate to show the effectiveness on the self-localization and the autonomous navigation than a differential wheel-based mobile robot. The extended Kalman filter consisting of an omnidirectional motion equation and the selective activation algorithm and a path-following control algorithm were presented. The results of experiments showed that the selective activation algorithm has better performances in terms of he self-localization and the autonomous navigation than the conventional global ultrasonic system with a simple sequential activation. The

https://doi.org/10.1017/S0263574707003888 Published online by Cambridge University Press

main reason is that the selective activation has much more valid ultrasonic data than the simple sequential activation.

As environmental objects can obstruct the ultrasonic signals, the performance of the selective activation algorithm could be improved by considering these obstacles. However, due to the large database requirements needed to address environmental objects, they were not considered here. Improvement can also be made by adding another criterion for selection of ultrasonic transmitter that gives the best posture estimation at a certain location.

Acknowledgments

The author would like to thank Yongtae Kim (Samsung Electronics), Jinwon Kim (Samsung Electronics), and Seongdo Kim (i3system) for their efforts on experiments. The author also appreciates anonymous reviewer's valuable comments.

References

1. S. Singh and P. Keller, "Obstacle detection for high speed autonomous navigation," *Proceedings of IEEE Int. Conf. on Robotics and Automation,* Sacramento, USA (September, 1991) pp. 2798–2805.
2. J. Leonard and H. Durrant-Whyte, *Directed Sonar Sensing for Mobile Robot Navigation* (Kluwer Academic Publishers, Cambridge, Massachusetts, 1992).
3. P. Sala, R. Sim, A. Shokoufandeh and S. Dickinson, "Landmark Selection for Vision Based Navigation," *Proceedings of IEEE/RSJ International Conference on Intelligent Robots and Systems (IROS2004)*, Sendai, Japan (September, 2004) pp. 3131–3138.
4. R. Want, A. Hopper, V. Falcao and J. Gibbons, "The Active Badge Location System," *ACM Trans. Inform. Syst.* **10**(1), 91–102 (1992).
5. S. Haihang, G. Muhe, and H. Kezhong, "An integrated GPS/CEPS position estimation system for outdoor mobile robot," *Proceedings of IEEE International Conference on Intelligent Processing Systems* Beijing, China (October, 1997) pp. 28–31.
6. S. Cobb, GPS Pseudolite: Theory, Design, and Application, *Ph.D.* Thesis (Stanford, CA: Stanford University, 1997).
7. C. Kee, H. Jun and D. Yun, "Indoor Navigation System Using Asynchronous Pseudolites," *J. Navig.* **56**, pp. 443–455 (2003).
8. J. Ko, W. Kim and M. Chung, "A Method of Acoustic Landmark Extraction for Mobile Robot Navigation," *IEEE Trans. Robot. Automat.* **12**(6), 478–485 (1996).
9. J. Leonard and H. Durrant-Whyte, "Mobile Robot Localization by Tracking Geometric Beacons," *IEEE Trans. Robot. Automat.* **7**(3), 376–382 (1991).
10. L. Kleeman, "Optimal Estimation of Position and Heading for Mobile Robots Using Ultrasonic Beacons and Dead-reckoning," *Proceedings of IEEE Conference on Robotics and Automations*, Nice, France (May, 1992) pp. 2582–2587.
11. http://www.hexamite.com/
12. N. Priyantha, A. Miu, H. Balakrishnan and S. Teller, "The Cricket Compass for context-aware mobile applications," *Proceedings of International Conference on Mobile Computing and Networking*, Rome, Italy (July, 2001) pp. 1–14.
13. S. Yi and B. Choi, "Autonomous Navigation of Indoor Mobile Robot Using Global Ultrasonic System," *Robotica* **22**(4), 369–374 (2004).
14. http://www.acroname.com/robotics/parts/R93-SRF04.html
15. G. Welch and G. Bishop, "An Introduction to the Kalman Filter," *Technical Report 95-041* (Chapel Hill, NC: University of North Caroline at Chapel Hill, 1995).
16. S. Ghidary, T. Tani, T. Takamori and M. Hattori, "A new Home Robot Positioning System (HRPS) using IR switched multi ultrasonic sensors," *Proceedings of IEEE International Conference on Systems, Man and Cybernetics,* Tokyo, Japan (October, 1999) pp. 737–741.